

Low-frequency resonance of moonpools

by J. N. Newman
<jnn@mit.edu>

(18th Workshop on Water Waves and Floating Bodies – Le Croisic, France – 6-9 April 2003)

Low-frequency ‘pumping’ modes are important for offshore structures with moonpools. In many cases the response is large and it is important to predict the resonant frequencies. Analyses of moonpools with vertical sides have been developed by Molin (2002), Tuck & Newman (2002), and others. Moonpools with cross-sections which vary with the depth are important in practical applications (Lee *et al*, 2002) and also for certain types of trapping structures (McIver & McIver 1997). Trapping structures with two moonpools have been studied recently by Shipway & Evans (2002) and by McIver & Newman (2002); for these cases there are two pumping modes, one corresponding to the pure trapping mode whereas the other radiates energy weakly to the far field. In numerical studies it is difficult to discriminate between these modes.

The objective here is to analyze the low-frequency resonant modes for moonpools with variable cross-sections. Linear potential theory is used. Two fundamental geometric assumptions are made: (a) the moonpools are slender vertically, with slowly-varying cross-sections, and (b) the fluid domain below the moonpools is bounded above by a rigid infinite plane, except for the openings into the moonpools. Coupling between multiple moonpools is included following the approach of Miles (2002). Three different examples are described: a simple torus with one moonpool, a structure with two isolated moonpools, and a structure with concentric moonpools. The estimates of the resonant wavenumber K are compared with computations of the added-mass coefficients, which are nearly-singular with pronounced zero-crossings at the same frequencies (Newman, 1999).

1 General analysis

The cross-sectional area $S_i(z)$ of each moonpool varies slowly between its bottom $z = z_b$ and the free surface $z = z_f$. The index $i = 1, 2, \dots$ is used to identify each moonpool and the subscripts f, b are used to denote values on the free surface (f) or bottom (b) of each moonpool. The vertical z -axis is positive upward. Assuming dS_i/dz is sufficiently small, the interior flow can be approximated by a quasi-uniform vertical velocity $w_i(z)$ throughout the corresponding moonpool. From continuity the volume flux $Q_i = w_i S_i$ is constant. Potential flow is assumed, with the linearized boundary condition

$$K\phi - \phi_z = 0 \tag{1}$$

applied on the free surface of each moonpool. Here $K = \omega^2/g$ is the wavenumber, ω is the frequency, and g denotes gravity. All hydrodynamic quantities are assumed to be harmonic in time with frequency ω .

The divergence theorem is applied to the fluid volume V_i in each moonpool. Thus

$$\int \int_{S_i} \phi \phi_n dS = \int \int \int_{V_i} (\nabla \phi)^2 dV \tag{2}$$

where the unit normal n is directed out of V_i . For the volume integral the assumption of quasi-uniform flow gives the relation

$$\int \int \int_{V_i} (\nabla \phi)^2 dV = \int_{z_b}^{z_f} w_i^2 S_i dz = w_{ib}^2 S_{ib}^2 \int_{z_b}^{z_f} \frac{dz}{S_i(z)} \quad (3)$$

The only contributions to the surface integral in (2) are from the upper and lower boundaries. Using (1) it follows that

$$\int \int_{S_{if}+S_{ib}} \phi \phi_n dS = \frac{S_{if} w_{if}^2}{K} - w_{ib} I_i = \frac{S_{ib}^2 w_{ib}^2}{K S_{if}} - w_{ib} I_i \quad (4)$$

Here the continuity condition $w_{ib} S_{ib} = w_{if} S_{if}$ has been used, and

$$I_i = \int \int_{S_{ib}} \phi dS \quad (5)$$

is the ‘impulse’ on S_{ib} . In $z \leq 0$ the potential can be expressed in the form

$$\phi(\mathbf{x}) = \frac{1}{2\pi} \sum_j w_{jb} \int \int_{S_{jb}} \frac{dS_\xi}{|\mathbf{x} - \xi|} \quad (6)$$

Substituting (3-6) in (2) gives the homogeneous linear system

$$w_{ib} S_{ib}^2 \left(\frac{1}{K S_{if}} - \int_{z_b}^{z_f} \frac{dz}{S_i} \right) - \sum_j w_{jb} I_{ij} = 0 \quad (7)$$

where

$$I_{ij} = \frac{1}{2\pi} \int \int_{S_{ib}} dS_{\mathbf{x}} \int \int_{S_{jb}} \frac{dS_\xi}{|\mathbf{x} - \xi|} \quad (8)$$

The eigenvalues of K determine the natural frequencies of the moonpools.

In the following examples the moonpools are axisymmetric, and the integrals (8) are evaluated analytically using well known integral relations for the source potential $1/|\mathbf{x} - \xi|$.

2 Torus with one moonpool

The moonpool occupies the circular domain $0 < r < R(z)$ about the vertical z -axis, and

$$I_{11} = \left(\frac{8}{3} \right) R_b^3 = \left(\frac{8}{3\pi} \right) S_b R_b \quad (9)$$

Substituting this result in (7) and solving for K it follows that

$$K = \left(S_f \int_{z_b}^{z_f} \frac{dz}{S(z)} + \frac{8R_b S_f}{3\pi S_b} \right)^{-1} \quad (10)$$

In the special case where $S(z) = \text{constant}$, this is consistent with Miles’ equation (3.3).

As examples we consider a cylinder with a moonpool of constant radius, and a torus with semi-elliptical submerged sections. Table 1 compares the estimates from (10) with computations for the same structures using WAMIT. For the torus with elliptical sections the estimate (10) overpredicts the resonant wavenumber, and the error increases as the moonpool radius is increased relative to the draft.

		cylindrical		elliptical	
r_{in}	r_{out}	(10)	WAMIT	(10)	WAMIT
0.25	1.25	0.824	0.835	1.466	1.407
0.5	2.5	0.702	0.721	1.328	1.174
1.0	5.0	0.541	0.568	1.118	0.846

Table 1: Value of the resonant wavenumber based on the approximation (10), compared with zero-crossings of the added mass from WAMIT. The cylindrical structure has vertical inner and outer surfaces and a flat bottom. The elliptical structure is a torus with semi-elliptical sections. The inner and outer radii at the free surface are listed in the first two columns. The draft is equal to 1.0.

3 Structure with two separated moonpools

Next we consider the structure shown in Figure 1, which includes two moonpools with their axes at $x = \pm c$. Except for the flat bottom between the moonpools the outer and inner sections are elliptical. The diagonal elements of (8) are evaluated from (9). The integrals for the off-diagonal elements can be evaluated in terms of the generalized hypergeometric series

$$I_{12} = \frac{\pi}{4} R_b^3 \beta \sum_{k=0}^{\infty} \frac{(\frac{3}{2})_k [(\frac{1}{2})_k]^2}{(3)_k (2)_k k!} \beta^{2k} \approx \frac{\pi}{4} R_b^3 \beta \quad (11)$$

where $\beta = R_b/c$ and $(a)_k = \Gamma(a+k)/\Gamma(a)$. In the range ($0 < \beta \leq 1$) where the moonpools do not overlap, the sum in (11) is nearly constant, increasing from 1.0 to 1.0888. Thus the ‘wide-spacing’ approximation in (11) is accurate within 9% throughout the relevant range.

The dimensions used for the structure in Figure 1 are $c = 1.5$, $R_b = 1$, $R_f = 0.5$, overall length=6, beam=3, and draft=1. For this geometry the roots of (7) give the resonant wavenumbers $K_1 = 0.987$ and $K_2 = 1.131$. These correspond respectively to symmetric and anti-symmetric pumping modes in the two moonpools. For comparison Figure 1 shows the heave and pitch added-mass coefficients of this structure for a range of wavenumbers. The points where these pass through zero values with large negative slope are at $K = 1.011$ and $K = 1.032$, respectively. Thus the agreement is within 2% for the symmetric mode and 10% for the antisymmetric mode.

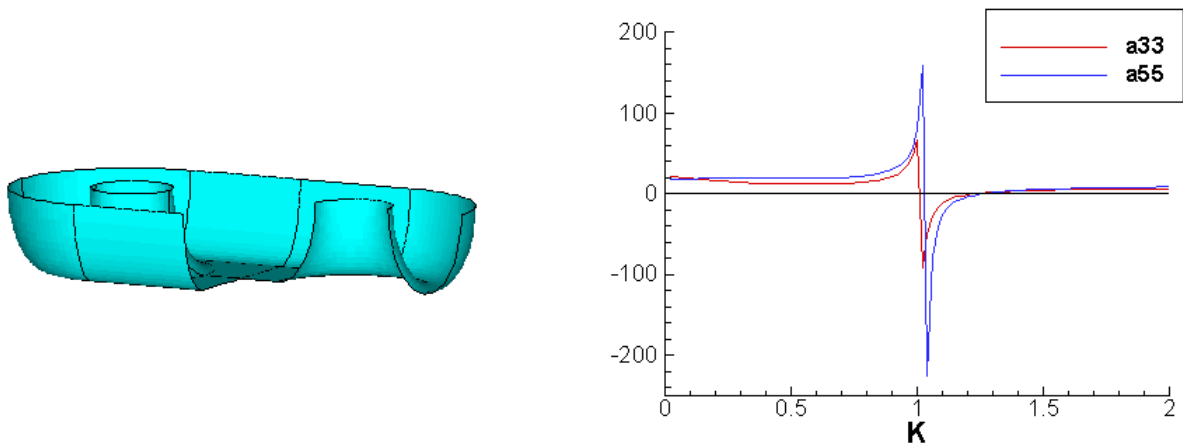


Figure 1: Structure with two separated moonpools. The perspective view on the left shows three of the four quadrants. The heave and pitch added-mass coefficients are plotted on the right.

4 Two concentric moonpools

Here we consider an example analogous to a trapping structure with two concentric annular moonpools. In this case the inertia coefficients can be expressed in terms of complete elliptic integrals. For the example shown in Figure 2 both toroids have semi-circular sections with radius 1, with the radii of their centers at 1.5 and 4. Three added-mass coefficients are shown including rigid-body heave of the entire structure, and two generalized modes which are more effective in forcing the in-phase and out-of-phase pumping motions between the two moonpools. The resonant wavenumbers for these two motions occur at $K = 0.860$ and $K = 1.193$ respectively, based on the zero-crossings. The corresponding roots of (7) are at $K_1 = 0.834$ and $K_2 = 1.438$.

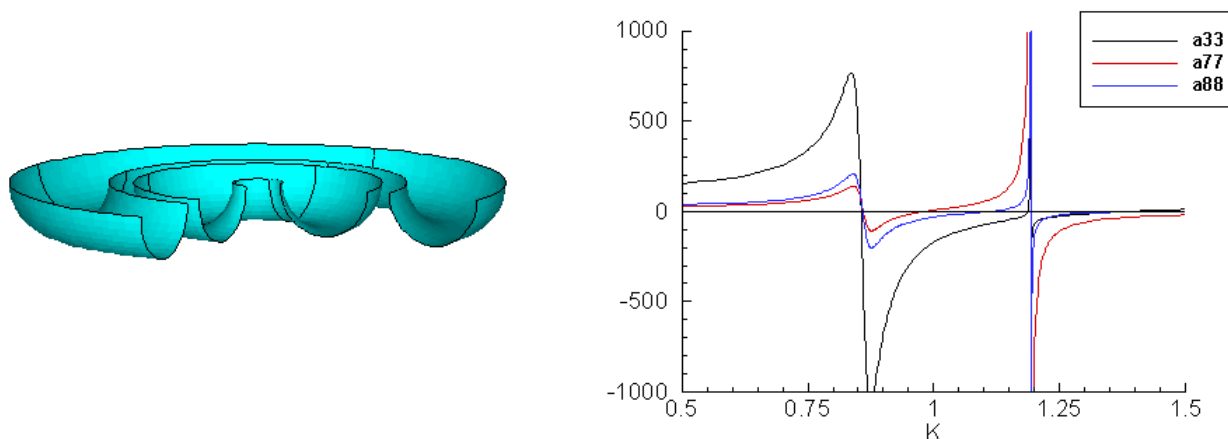


Figure 2: Structure with two concentric moonpools. The perspective view on the left shows three of the four quadrants. The plot on the right shows the added-mass coefficients for heave of the entire structure (a_{33}), heave of the inner torus alone (a_{77}), and radial motion of the inner structure (a_{88}).

REFERENCES

- Lee, C.H., Letcher, J.S., Mack, R.G., Newman, J.N. & Shook, D.M. 2002 Integration of geometry definition and wave analysis software, *Proc. 21st Intl. Conference on Offshore Mechanics and Arctic Engineering*, Oslo, Norway.
- McIver, P. & McIver, M. 1997 Trapped modes in an axisymmetric water-wave problem, *Q. Jl Mech. appl. Math.* **50**, 165–178.
- McIver, P. & Newman, J.N. 2002 Trapping structures in the three-dimensional water-wave problem, *J. Fluid Mech.* (in press).
- Miles, J. 2002 On slow oscillations in coupled wells, *J. Fluid Mech.* **455**, 283–287.
- Molin, B., 2001 On the piston and sloshing modes in moonpools, *J. Fluid Mech.* **430**, 27–50.
- Newman, J.N., 1999 Radiation and diffraction analysis of the McIver toroid, *J. Engng. Math.* **35**, 135–147.
- Shipway, B.J. & Evans, D.V. 2002 Wave trapping by axisymmetric concentric cylinders, *Proc. 21st Intl. Conference on Offshore Mechanics and Arctic Engineering*, Oslo, Norway.
- Tuck, E.O. & Newman, J.N. 2002 Longitudinal sloshing in slender moonpools, *Proc. 17th Intl. Workshop on Water Waves and Floating Bodies*, Cambridge, UK.